Adsorbate–adsorbate repulsions—the coverage dependence of the adsorption structure of CO on Cu(110) as studied by electronstimulated desorption ion angular distribution

Joachim Ahner, Dan Mocuta, R. D. Ramsier, and John T. Yates Jr.

Citation: The Journal of Chemical Physics **105**, 6553 (1996); doi: 10.1063/1.472464
View online: http://dx.doi.org/10.1063/1.472464
View Table of Contents: http://scitation.aip.org/content/aip/journal/jcp/105/15?ver=pdfcov
Published by the AIP Publishing

Adsorbate–adsorbate repulsions—the coverage dependence of the adsorption structure of CO on Cu(110) as studied by electron-stimulated desorption ion angular distribution

Joachim Ahner
Department of Chemistry, University of Pittsburgh, Surface Science Center, Pittsburgh, Pennsylvania 15260

Dan Mocuta and R. D. Ramsier
Department of Physics and Astronomy, University of Pittsburgh, Pittsburgh, Pennsylvania 15260

John T. Yates, Jr.
Department of Chemistry, University of Pittsburgh, Surface Science Center, Pittsburgh, Pennsylvania 15260

(Received 15 March 1996; accepted 1 July 1996)

The coverage dependent orientation of CO adsorbed on a Cu(110) surface was studied by the electron-stimulated desorption ion angular distribution (ESDIAD) technique. A neutral excited (CO^*) species is imaged and in addition positive ions are measured. The adsorption temperature was varied between 32 K and 150 K. By applying the ESDIAD technique at a temperature below 80 K it was possible to decrease the beamwidths drastically, to determine the angular distributions better than $\pm 0.5°$, and to study the adsorption of CO chemisorbed and physisorbed on the surface. With increasing CO coverage we observe three distinct ESDIAD patterns. Starting from a normal beam pattern with an elliptical cross section with the major axis oriented in the $\langle 110 \rangle$ direction for coverages up to 0.2 monolayer (ML), a transformation of the ESDIAD pattern into a pattern of two separated beams is observed for a coverage of about 0.5 ML, indicating a tilting of the molecules in the $\langle 110 \rangle$ directions by $\sim 9°$. With further increasing CO coverage an additional central peak develops with an elliptical broadening now in the $\langle 001 \rangle$ direction. The changes of the pattern are reversible as shown by decreasing the coverage by thermal desorption. Based on these ESDIAD and digital low energy electron diffraction results, a linear-chain model for CO adsorption is proposed. Temperature programmed desorption measurements also indicate the presence of repulsive CO–CO interactions in the adlayer. © *1996 American Institute of Physics.* [S0021-9606(96)00238-3]

I. INTRODUCTION

Electron-stimulated desorption ion angular distribution (ESDIAD) has been shown to be a rather direct method of determination of adsorbate orientation. Its principles and applications have been reviewed extensively by Ramsier and Yates,[1] Madey,[2] and Menzel.[3] Although the very direct connection between the observed angular distribution of the desorbing ions or excited neutrals depends on the applicability of several simplifying assumptions,[2,4–6] in principle it is clear that the ESDIAD angular distributions contain contributions from the ground state orientation convoluted with image force deflection[7] and other final-state effects, as well as from adsorbate vibrations.[4]

The interaction of CO with metal surfaces has been studied extensively in the past with many different kinds of surface science methods.[8,9] Many studies have focused on the structure and the electronic properties of CO chemisorbed on transition metal surfaces.[8] Many of these investigations indicate that at higher coverages interactional effects begin to control the structural character of the chemisorbed CO. For example, in the cases of CO/Ni(110),[5,10] CO/Pt(111),[11,12] and CO/Ru(0001),[5] repulsive interactions cause tilting of the CO from the normal orientation as the coverage is increased.

CO adsorption on Cu(110) has been studied for adsorption temperatures higher than 90 K and coverages less than $\theta = 0.5$ ML. A CO-induced (2×1) LEED superstructure has been reported.[13–15] For coverages up to $\theta = 0.5$ ML it has been shown through angular resolved photoelectron spectroscopy[16] that the CO bond axis is perpendicular to the macroscopic surface plane. Recently this was confirmed through photoelectron diffraction measurements from which an atop position of the adsorbed CO molecule and a Cu–C separation of 1.9 Å has been determined.[17] The uncertainty for the angles between Cu, C, and O obtained by this method is declared to be not better than $\pm 5°$.[17]

There exist no ESDIAD data on the CO/Cu(110) system in the literature to our knowledge, as well as no data showing the orientation of the Cu–CO bond axis for CO-coverages above 0.5 ML or at temperatures below 80 K. This paper focuses on the CO adsorption structure and the carbon–metal bond orientation for coverages which extend into the multilayer regime.

II. EXPERIMENT

The experiments were performed in an UHV chamber with a base pressure below 1×10^{-10} mbar, which was described previously.[10,18] The Cu single crystal,[19] a cylindrical

disk 3 mm thick, with a diameter of 10 mm, could be cooled down to 85 K by using liquid nitrogen and heated up to 900 K by resistive heating.

With the intention to get lower temperatures the following two methods were applied: (1) He gas was bubbled through l-N_2 held in the manipulator body, reaching a temperature of 73 K.[20] (2) To lower the temperature further it was necessary to use l-He for cooling. Therefore we modified our homebuilt liquid nitrogen bath cryostat and designed a special transfer tube for the l-He. By using a stainless steel delivery tube with an inner diameter of only 1 mm, surrounded by an insulating vacuum jacket, it was possible to produce crystal temperatures as low as 32 K. The cooling system works as a constant flow rate He cryostat. By applying different pressures, the flow rate could be adjusted between 0.05 ℓ/min and 0.2 ℓ/min. For a typical flow rate of 0.1 ℓ/min the cooling time for the crystal fom 860 K to 32 K was only 15 min.

A type-K thermocouple was used for temperature measurements. The absolute temperature reading is limited by the accuracy of the thermocouple voltage, which has an error of ± 3 K in the temperature range between 30 and 40 K.[21] By adsorbing multilayers of CO at different temperatures and CO partial pressures and comparing with the literature values of the CO vapor pressure[22] the lowest temperature was determined to be 32 K (± 2 K).

After continuing cycles of Ar ion sputtering (40 min at 300 K with an ion energy of 1000 eV and an ion current of 1 μA) and subsequent annealing to 860 K for 5 min, the cleanliness of the Cu surface was examined by Auger electron spectroscopy (AES). The main impurities sulphur, oxygen, and carbon were found to be smaller than the detection limit of the cylindrical mirror analyzer (CMA) in the depth of sampling of AES (<0.001 ML). In addition, a sharp (1×1) LEED pattern was obtained.

The crystal was exposed to CO either by a calibrated beam doser[23,24] or by isotropic dosing from the background. Because of the uncertainty in the position of the crystal in front of the doser and in the exact angular distribution of the gas molecules leaving the doser, the accuracy errors of the exposure and hence the absolute CO coverage may be much larger than the high precision (4%) of the doser itself.[24] The accuracy in determining the coverage from background dosing is limited by the uncertainty in the CO pressure reading. The relative coverages are of an accuracy of $\pm 2\%$ as measured by integrating the temperature programmed desorption (TPD) peaks.

The digital ESDIAD apparatus has been described in detail before.[25] The grid potentials in the ESDIAD apparatus have been adjusted to retard both positively and negatively charged particles. Thus, only excited neutral CO* species are observed by the MCP detector. This species originating from Cu(110) has not been identified and may be $a^3\pi$-CO (Ref. 26) or CO in highly excited vibrational states,[27] or a mixture of the two excited species. The trajectories of these neutral CO* species will not be influenced by image charge effects at the Cu surface. Since a Chevron-type multichannel plate (MCP) is used, a slightly reduced gain for photons and excited neutrals hitting the MCP at the tilting angle of the capillaries (compare Ref. 28) has been observed.

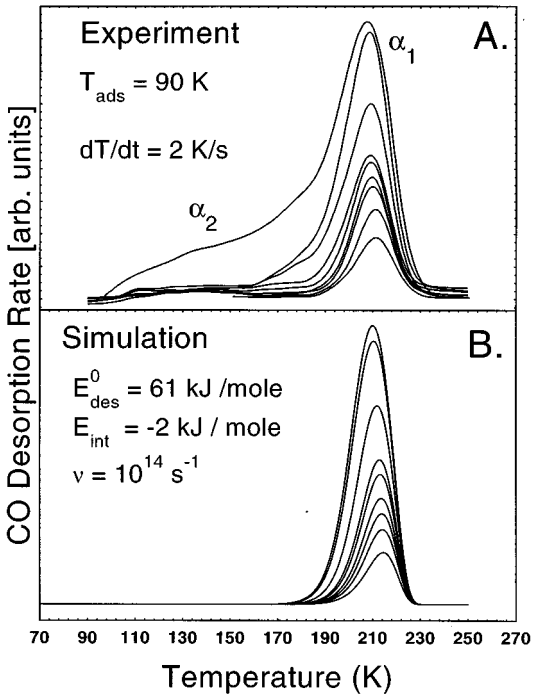

FIG. 1. (Upper graph) Thermal desorption spectra of CO from Cu(110) after initial CO coverages from $\theta=0.06$ ML to 0.8 ML at 90 K; heating rate $dT/dt=2$ K/s. (Lower graph) Numerically created TPD-spectra of the α_1 state on the basis of the Polanyi–Wigner equation. From the best fit to the experimental data values for the pre-exponential factor of $\nu_0=10^{14}$ s^{-1} and for the zero coverage desorption energy $E^0_{des}=61$ kJ/mol and for the coverage dependent adsorbate interaction energy of $E_{int}=-2$ kJ/mol are obtained.

III. RESULTS

A. Temperature programmed desorption of CO chemisorbed on Cu(110)

Figure 1(a) shows a typical set of TPD spectra of CO after different CO exposures at 90 K. Only molecular CO could be detected as a desorbing product. It can be seen [Fig. 1(a)] that at CO coverages up to 0.5 ML only the α_1 peak appears. The peak maxima shifted slightly to lower temperatures with increasing initial CO coverages. As the CO coverage was increased, a shoulder appeared on the low temperature edge and formed an additional relatively broad peak, α_2. The steepness of the low temperature edge for high coverages at 90 K indicated that the adsorption state, α_2, is not saturated.

Figure 1(b) shows an optimized fit of spectra created numerically on the basis of the Polanyi Wigner equation,

$$R_{des}=\nu\cdot\frac{1}{\beta}\cdot\theta\cdot\exp[-(E^0_{des}+E_{int}\cdot\theta)/kT], \tag{1}$$

where R_{des} is the desorption rate, expressed as $d\theta/dT$, ν the frequency factor, $\beta=dT/dt$, E^0_{des} the zero coverage desorption activation energy, and E_{int} the interaction energy of the adsorbates. The numerical creation of the spectra was done

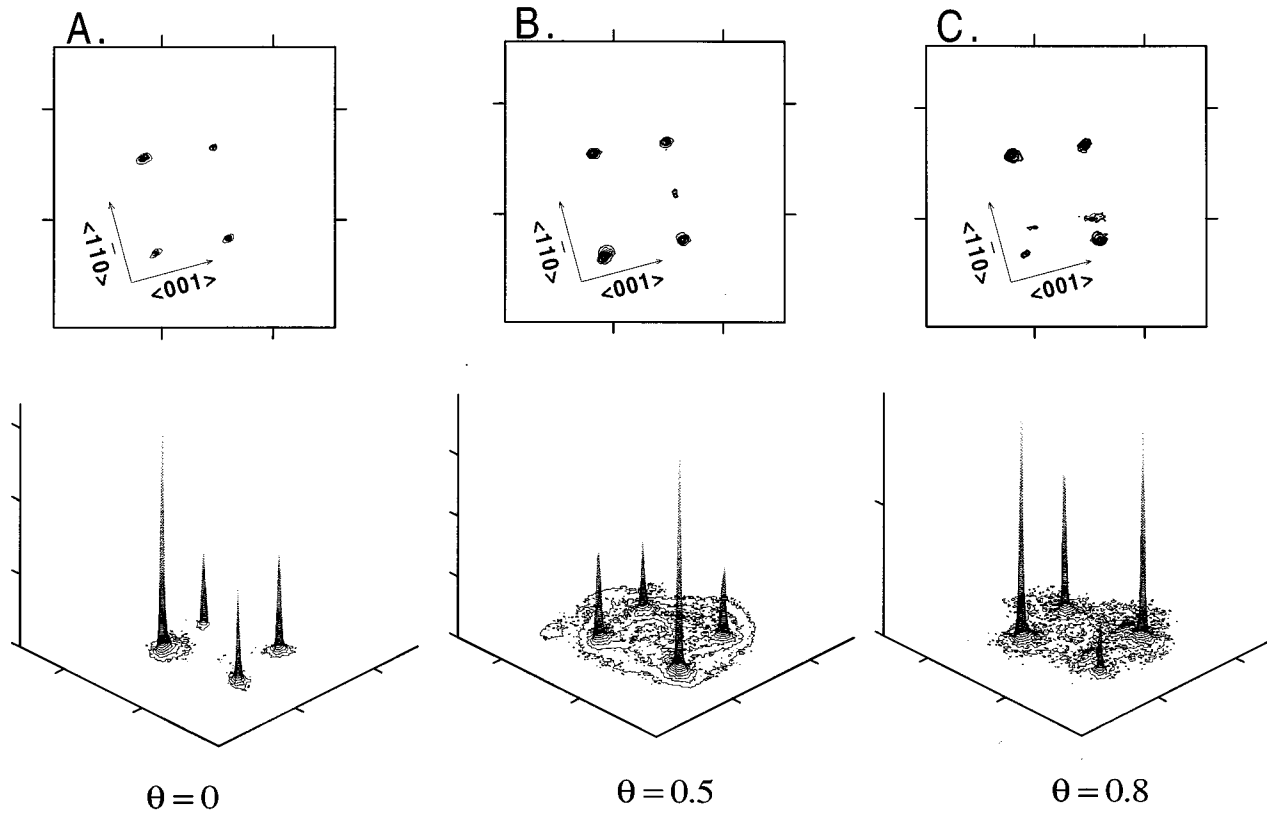

FIG. 2. LEED patterns of the clean Cu(110) surface and of two different CO coverages at a temperature of 90 K. The (2×1) superstructure could be seen only very weakly for a CO coverage of θ=0.5 ML, as well as the streaky (5/4×2) structure for a coverage of θ=0.8 ML.

by a home written computer program using a Runge Kutta routine and a least square fitting to the experimental data with ν, $E^0_{\rm des}$, and $E_{\rm int}$ as free parameters.

From the optimal fit the following values are obtained: $\nu=10^{14}$ s^{-1}; $E^0_{\rm des}$=61 kJ/mol; and $E_{\rm int}=-2$ kJ/mol. The negative value for $E_{\rm int}$ indicates the presence of repulsive adsorbate interactions with increasing coverage. These results are in good agreement with the TPD results for CO on Cu(110) of Christiansen *et al.*[29] for low CO coverages. They obtained for the α_1 peak a desorption energy of 58 kJ/mol. In contrast to their interpretation, the simulation of the TPD spectra shows that the appearance of the low temperature α_2 peak cannot be explained by a slight increase of the repulsive adsorbate interaction deduced from the behavior of the α_1 state. Instead, a large change in binding energy must occur as α_2-CO is populated.

B. LEED results

All of the former LEED observations on the system CO/Cu(110) (Refs. 13, 15, 29) used conventional LEED instruments, which operate with electron current densities in the range of several μA/mm^2. In contrast to this, in the work presented here, LEED data were taken with the digital LEED/ESDIAD instrument at an electron current density of only 1 nA/mm^2. This is an important point when comparing the LEED data, since electron bombardment on the adlayer might have influenced the results. It is well known that electrons in the energy range of the LEED measurements (typically 40 eV–200 eV) could cause electron stimulated desorption,[1,3] dissociation,[30] and migration[31,32] of adsorbed species.

Typical LEED patterns obtained with the digital ESDIAD/LEED instrument at an electron energy of 100 eV are presented in Fig. 2. For the clean Cu(110) surface a (1×1) electron diffraction pattern is observed as shown in Fig. 2(a). The very narrow first order diffraction peaks and the low background indicate a flat and smooth (110) surface of the fcc crystal. The azimutal ⟨001⟩ orientation of the crystal was inclined 13° with respect to the horizontal axis.

The Cu(110) surface at 80 K was filled to about half a monolayer of CO (only the α_1-state is filled; compare with Fig. 1). In addition to the well pronounced (1×1) diffraction peaks and an increased background intensity, only very weak additional diffraction beams were observed. These additional beams indicate a poorly-ordered (2×1) superstructure [Fig. 2(b)]. Subsequent annealing to temperatures up to 170 K and cooling down again did not change this very weak (2×1) structure. This observation is in contrast to the former LEED reports on the CO/Cu(110) system[13,15,29] which describe a clear (2×1) LEED pattern at a CO coverage of θ=0.5 ML.

After increasing the CO coverage at 80 K, a weak streaky (5/4×2) structure is observed [Fig. 2(c)]. This superstructure is also only very weakly pronounced and appears on an increased background. Subsequent heating to 170 K and cooling down again revealed the very weak (2×1) structure.

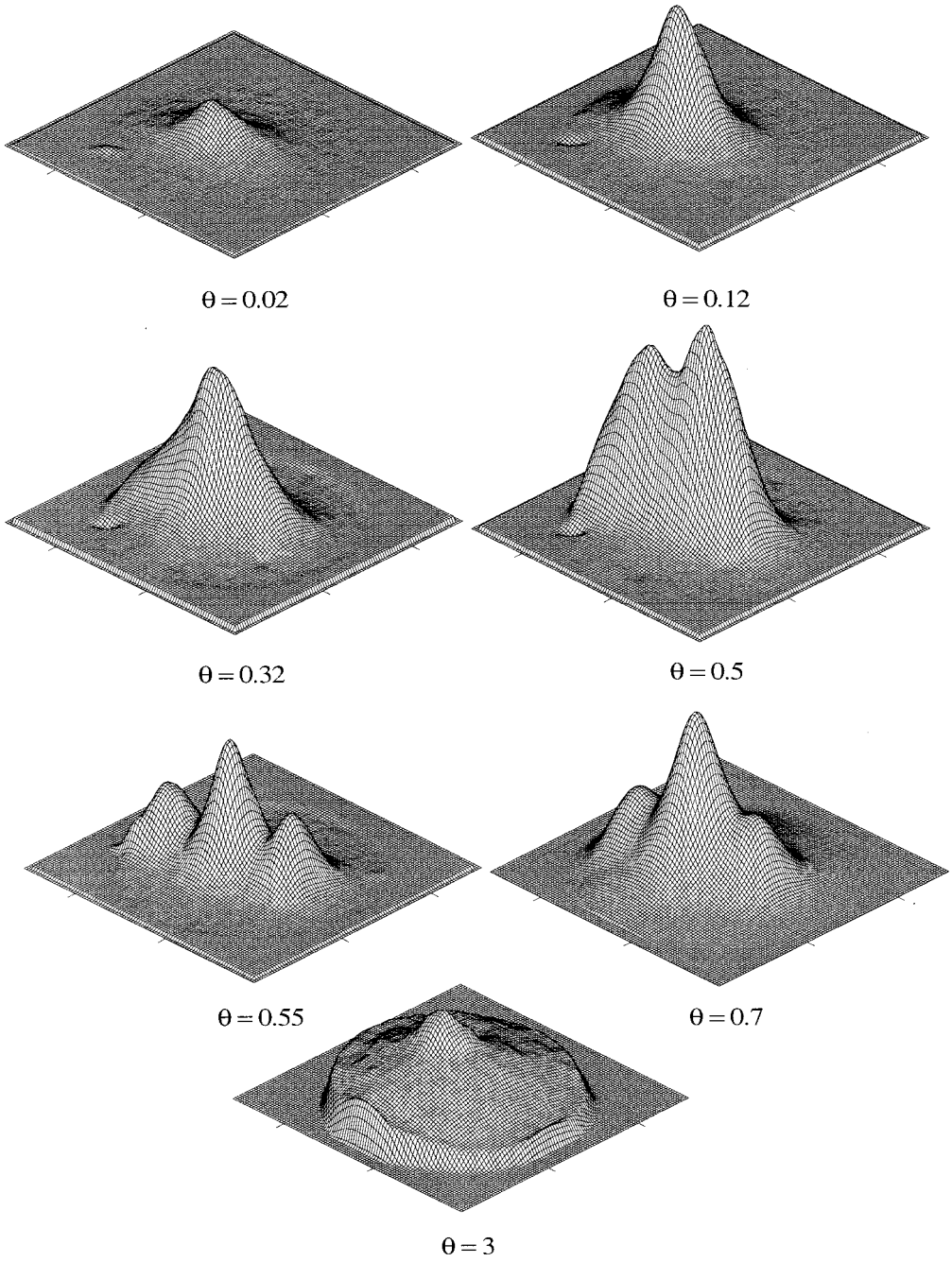

FIG. 3. CO* ESDIAD patterns obtained for different CO coverages on Cu(110) at $T=32$ K, presented in a three-dimensional surface plot.

C. ESDIAD results

Figure 3 shows a representative selection of CO* ESDIAD patterns obtained at different CO coverages and at an impinging electron energy of 200 eV. As in Fig. 2, the ⟨001⟩ direction is inclined 13° with respect to the horizontal x axis. Changing of the electron energy over the range 90–600 eV had almost no influence on the ESDIAD pattern. The patterns for CO coverages up to $\theta=0.12$ are almost identical in shape, showing a linear increase of the integrated yield of CO* species with the CO coverage. A single normal elliptical ESDIAD beam is seen with the long axis of the ellipse oriented parallel to the rows of Cu atoms. This may be seen clearly in Fig. 4, where contour plots of the data of Fig. 3 are shown. With increasing coverage, the intensity of this normal ESDIAD beam decreased. At the same time on both ends of the long axis of the ellipse, additional beams began to grow steadily as shown in Fig. 3 for a CO coverage of $\theta=0.32$. At a coverage of $\theta=0.5$ the normal ESDIAD beam disappeared totally and only the two ESDIAD beams were seen. They are tilted symmetrically 9° from the surface normal in the ⟨110⟩ direction (parallel to the rows of the Cu atoms). This is demonstrated in Fig. 5, where line cuts in the ⟨110⟩ direction through the presented ESDIAD patterns are shown. After increasing the CO coverage by only a small

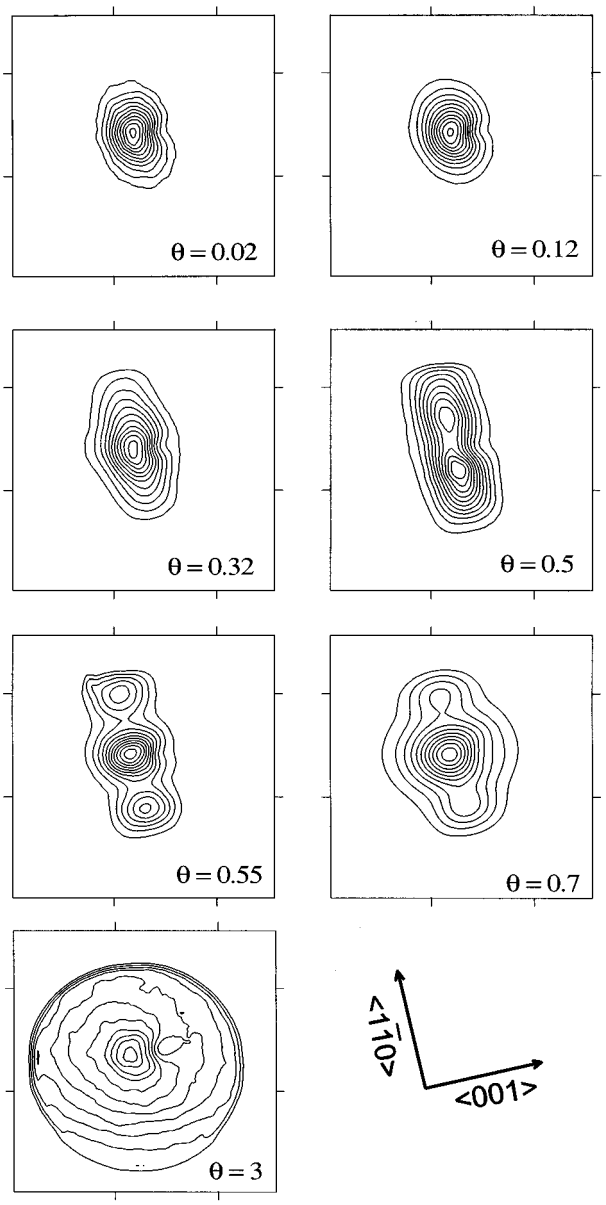

FIG. 4. Identical CO* ESDIAD results as in Fig. 3, but presented in a two-dimensional contour plot. Comparison with Fig. 2 shows that the two and three beam ESDIAD patterns are orientated parallel to the ⟨110⟩ azimuthal direction of the Cu(110) surface.

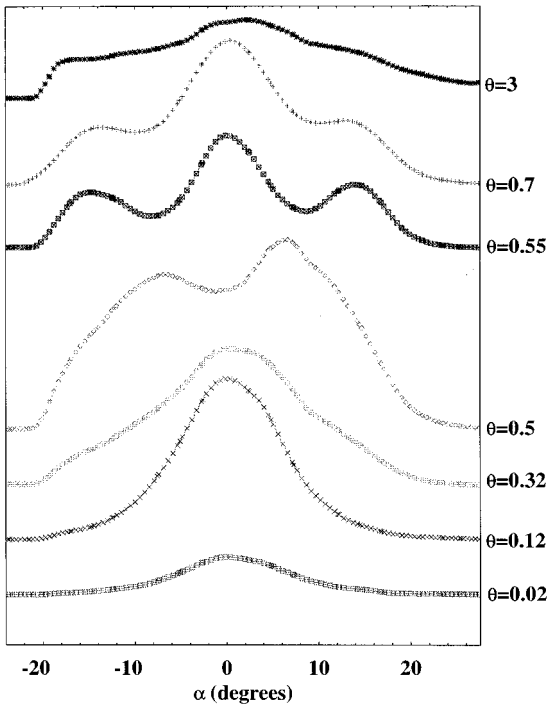

FIG. 5. Line-cuts through the CO* ESDIAD patterns of Figs. 3 and 4 in the ⟨110⟩ direction for different CO coverages on Cu(110) at $T=32$ K. The stepwise change of the pattern shapes at about $\theta=0.5$ ML indicates a phase transition in a narrow coverage range.

amount, the two-beam pattern changed stepwise into a three-beam pattern as shown in Fig. 3, 4, and 5 for a CO coverage of $\theta=0.55$. The normal beam is slightly elliptical in shape, now with the long axis of the ellipse oriented perpendicular to the rows of Cu atoms. The other two beams were tilted symmetrically 16° from the surface normal in a plane parallel to the rows of Cu atoms. With further increasing coverage up to one monolayer the normal beam intensifies with increasing elliptical anisotropy in the ⟨100⟩ direction, while the tilted beams decrease slightly in intensity. We estimate from the shape of the ellipse that the maximum tilt angles in the ⟨001⟩ directions are no more than 2.5°. At a CO coverage corresponding to a three monolayer exposure the normal ESDIAD beam is reduced in intensity and is superimposed on an intense featureless background signal. The background signal may indicate random orientation of CO molecules in the multilayer.

The changes of these coverage dependent ESDIAD patterns were reversible as demonstrated by decreasing the coverage by thermal desorption and cooling down again to 32 K.

The ESDIAD pattern at the same CO coverage and temperature conditions but with no retarding electrical field for positive ions were recorded. By subtracting the CO* ESDIAD pattern from these data, it was possible to obtain the ESDIAD pattern also for positive ions (CO^+ and O^+). The results indicated almost the same behavior with a decreased total yield by a factor of 2.

IV. DISCUSSION

These experimental observations are the basis of a simple model for the adsorption of CO on Cu(110) as proposed in Fig. 6 where a sequence of linear chain structures for CO is shown for increasing CO coverage in the left-hand pattern. At low CO coverages the CO molecules, adsorbed on the atop sites of the surface Cu atoms with a normal orientation of the Cu–CO axis, are isolated from nearest neighbors by adsorbate repulsion. With increasing CO coverage and hence increasing adsorbate interaction, pairs of neighboring chemisorbed CO molecules begin to form with tilting of the molecules in the ⟨110⟩ directions due to repulsive nearest neighbor interaction. At a critical CO coverage of about $\theta=0.5$, the CO pairs aggregate together forming chains of at least four chemisorbed CO molecules along the

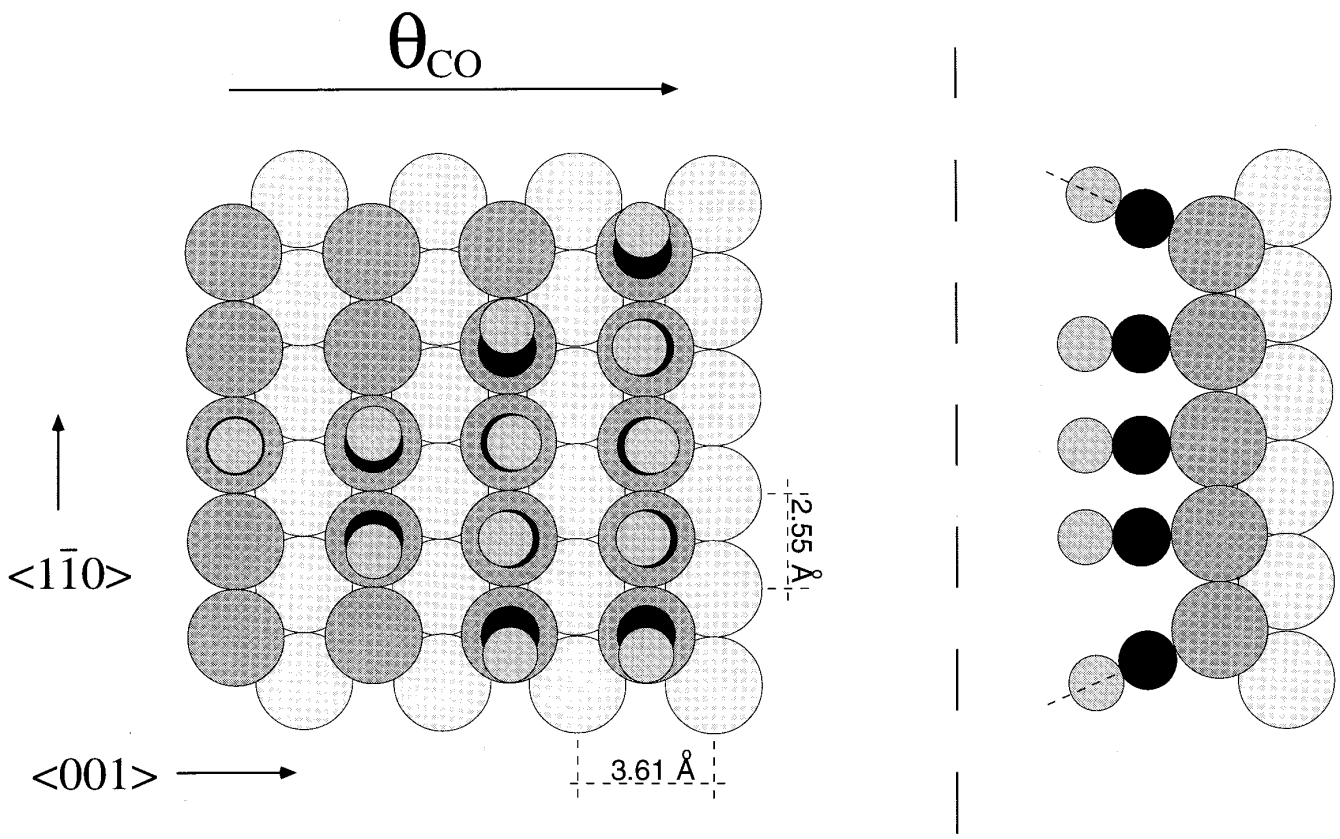

FIG. 6. Linear chain model for the adsorption of CO on Cu(110), schematically shown for increasing coverage moving from left to right.

$\langle 1\bar{1}0\rangle$ directions. Since the repulsive forces on the central molecules in these chains are now from two opposite directions, the central CO molecules become almost normally oriented and are now slightly tilted in the $\langle 001\rangle$ directions forming the elliptical normal ESDIAD beam with its long axis now orthogonal to the original long elliptical axis for CO at low coverages. The two more highly tilted ESDIAD beams are formed by the tilted CO molecules chemisorbed at the ends of the chains where adjacent empty sites permit 16° tilting. With further increasing coverage the length of the chains increases and, as a consequence of the increasing number of CO molecules chemisorbed in the center of the chains, the intensity of the almost normal ESDIAD beam increases. Similar coverage dependent orthogonal tilting phenomena have also been observed for CO adsorbed on the step sites of Pt(112).[33] The fact that the normal ESDIAD beam could be seen up to a CO exposure of three monolayers give evidence for a Vollmer–Weber growth mode under these adsorption conditions.

It is of interest to compare these results to similar studies of CO chemisorption on Ni(110).[5,10,34–38] In the case of Ni(110), it was observed that CO molecules at low coverages initially adsorbed with a normal Ni–CO bond orientation, as also seen for Cu(110). For Ni(110), as the CO coverage was increased, intermediate configurations with CO molecules tilted along the atom row direction were not seen; instead the configuration formed involved the production of CO species in an ordered p2mg overlayer and inclined ±19° in the $\langle 001\rangle$ directions. Thus, comparing Cu(110) to Ni(110), four significant experimental differences are observed.

(1) CO on Cu(110) does not form an ordered overlayer, whereas CO on Ni(110) is highly ordered, based on LEED studies.
(2) CO on Cu(110) is more weakly bound than CO on Ni(110). For Cu, $E^0_{\rm des}$=61 kJ/mol; for Ni, $E^0_{\rm des}$=128 kJ/mol.[38]
(3) CO on Cu(110) produces intermediate configurations proposed to be due to island chains of CO molecules separated by vacancy sites and undergoing repulsive interactions which produce a sequence of orthogonally tilted structures. CO on Ni(110) produces only the initial (normal) and final $\langle 001\rangle$ tilted configurations observed for Cu.
(4) The tilted CO species on Cu(110) for the most crowded condition exhibit ±2.5° tilting in the $\langle 001\rangle$ directions. On Ni(110) in the most crowded condition, the comparable tilt angle is ±19°.

Two factors may explain these differences.

(1) Because CO on Cu(110) is less strongly chemisorbed than on Ni(110), the occupancy of the CO-2π* orbitals is less for CO/Cu(110) compared to CO/Ni(110). This is in good agreement with recent two-photon photoemission (2PPE) results[39] and theoretical modeling of the CO–metal bond[40–43] which demonstrate that the CO–

surface bond is dominantly formed by the interaction of the 5σ and $2\pi^*$ orbitals with the sp conduction band rather than with the d conduction band as believed in the traditional picture, the Blyholder model.[44] Thus space-filling electronic charge located off the C–O bond axis is smaller for CO/Cu than for CO/Ni.

(2) The Cu–Cu interatomic spacing along the rows of Cu atoms is 2.556 Å, larger than the comparable Ni–Ni spacing of 2.492 Å.

Both of these factors—$2\pi^*$ orbital occupancy and substrate atom spacing would argue that CO–CO repulsive interactions due to CO···CO orbital overlap would be less for Cu(110) compared to Ni(110). In addition, the weaker metal–CO bonding for Cu(110) and the absence of strong ordering, argues that pinning of CO molecules to the lattice is less favorable for Cu(110) compared to Ni(110). The CO molecules can adjust their sites in accordance with the repulsive interactions on Cu(110) more than on Ni(110). Long range ordering does not occur on Cu(110) because of the vacancy sites which are formed by lateral motion during the filling of the surface. Thus a sequence of tilted configurations is observed on Cu(110) in an essentially long range disordered layer.

In addition, in the most highly crowded situation seen for the two metals, the large tilt angles in the $\langle 001 \rangle$ direction for Ni(110) ($\pm 19°$) compared to Cu(110) ($<2.5°$) are consistent with enhanced CO-$2\pi^*$ orbital occupancy and the smaller lattice spacing for Ni(110) compared to Cu(110), leading to larger CO···CO repulsive forces.

V. CONCLUSIONS

CO chemisorption on Cu(110) involves the production of a sequence of local surface configurations as the coverage is increased. The configurations involve orthogonal CO tilt directions reflecting the balance of CO···CO repulsive interactions in disordered island chains of chemisorbed CO molecules, separated by vacancy sites, even at the highest coverage achieved at a crystal temperature of 32 K. A comparison to comparable studies on Ni(110) reveals that the differences in the sequence of CO tilting configurations are consistent with the larger CO···CO repulsion on Ni(110) than on Cu(110) due to more extensive $2\pi^*$ orbital occupancy and smaller lattice spacing for CO/Ni(110) compared to CO/Cu(110).

ACKNOWLEDGMENT

Support of this work by the Office of Basic Science of the Department of Energy is gratefully acknowledged.

[1] R. D. Ramsier and J. T. Yates, Jr., Surf. Sci. Rep. **12**, 243 (1991).
[2] T. E. Madey, F. P. Netzer, J. E. Houston, D. M. Hanson, and R. Stockbauer, in *Desorption Induced by Electronic Transitions. DIET 1*, edited by N. H. Tolk, M. M. Traum, T. C. Tully, and T. E. Madey (Springer, Berlin, 1983), p. 120; T. E. Madey, C. Benndorf, N. D. Shinn, Z. Miskovic, and J. Vukanic, in *DIET II*, edited by W. Brenig and D. Menzel (Springer, Berlin, 1985), p. 104; T. E. Madey and R. Stockbauer, in *Methods in Experimental Physics*, edited by R. L. Park and M. G. Lagally (Academic, New York, 1985), Vol. 22, p. 465.
[3] D. Menzel, Nucl. Instrum. Methods B **101**, 1 (1995).
[4] J. T. Yates, Jr., M. D. Alvey, M. J. Dresser, M. A. Henderson, M. Kiskinova, R. D. Ramsier, and A. Szabo, Science **255**, 1397 (1992); T. E. Madey, *ibid.* **234**, 316 (1986).
[5] W. Riedl and D. Menzel, Surf. Sci. **207**, 494 (1989).
[6] W. L. Clinton, Phys. Rev. Lett. **39**, 965 (1977).
[7] Z. Miscovic, J. Vukanic, and T. E. Madey, Surf. Sci. **141**, 285 (1984); **169**, 405 (1986).
[8] J. C. Campuzano, *The Adsorption of Carbon Monoxide by the Transition Metals*, in Vol. 3 of *The Chemical Physics of Solid Surfaces and Heterogeneous Catalysis*, edited by D. A. King and D. P. Woodruff (Elsevier, Amsterdam, 1990), Part A, p. 389.
[9] J. T. Yates, Jr., Surf. Sci. **299/300**, 731 (1994).
[10] M. D. Alvey, M. J. Dresser, and J. T. Yates, Jr., Surf. Sci. **165**, 447 (1986).
[11] M. Kiskinova, A. Szabó, A-M. Lanzillotto, and J. T. Yates, Jr., Surf. Sci. **202**, L559 (1988).
[12] Kiskinova, A. Szabó, and J. T. Yates, Jr., Surf. Sci. **205**, 215 (1988).
[13] K. Horn, M. Hussain, and J. Pritchard, Surf. Sci. **63**, 244 (1977).
[14] A. Spitzer and H. Lüth, Surf. Sci. **102**, 29 (1981).
[15] Harendt, J. Goschnick, and W. Hirschwald, Surf. Sci. **173**, 176 (1986).
[16] E. Holub-Krappe, K. C. Prince, K. Horn, and D. P. Woodruff, Surf. Sci. **173**, 176 (1986).
[17] K.-M. Schindler, Ph. Hofmann, V. Fritzsche, S. Bao, S. Kulkarni, A. M. Bradshaw, and D. P. Woodruff, Phys. Rev. Lett. **71**, 2054 (1993); Ph. Hofmann, K.-H. Schindler, S. Bao, V. Fritsche, A. M. Bradshaw, and D. P. Woodruff, Surf. Sci. **337**, 169 (1995).
[18] M. D. Alvey, M. J. Dresser, and J. T. Yates, Jr., J. Vac. Sci. Technol. A **4**, 1446 (1986).
[19] The crystal was obtained from the KFA Juelich, and is oriented to within 0.05° of the [110] direction.
[20] J. Xu, H. J. Jänsch, and J. T. Yates, Jr., J. Vac. Sci. Technol. A **11**, 726 (1993).
[21] H. Schlichting and D. Menzel, Rev. Sci. Instrum. **56**, 2013 (1994).
[22] *Handbook of Chemistry and Physics*, 74th ed., edited by D. R. Lide and H. P. R. Frederikse (Chemical Rubber, Cleveland, 1994).
[23] M. J. Bozack, L. Muehlhoff, J. N. Russell, Jr., W. J. Choyke, and J. T. Yates, Jr., J. Vac. Sci. Technol. A **5**, 1 (1987).
[24] V. S. Smentkowski and J. T. Yates, Jr., J. Vac. Sci. Technol. A **7**, 3325 (1989).
[25] J. T. Yates, Jr., M. D. Alvey, K. W. Kolasinski, and M. J. Dresser, Nucl. Instrum. Methods Phys. Res. B **27**, 147 (1987).
[26] A. R. Burns, E. B. Stechtel, and D. R. Jennison, Phys. Rev. Lett. **58**, 250 (1987).
[27] S. Wurm, P. Feulner, and D. Menzel, Phys. Rev. Lett. **74**, 2591 (1995).
[28] M. B. Corbett and A. Then, in *The Photonics Design and Applications Handbook* (1994), H-110.
[29] M. Christiansen, E. V. Thomsen, and J. Onsgaard, Surf. Sci. **261**, 179 (1992).
[30] R. D. Ramsier, M. A. Henderson, and J. T. Yates, Jr., Surf. Sci. **257**, 9 (1991).
[31] H. J. Jänsch, J. Xu, and J. T. Yates, Jr., J. Chem. Phys. **99**, 721 (1993).
[32] A. G. Fedorus, E. V. Klimenko, A. G. Naumovets, E. M. Zasimovich, and I. N. Zasimovich, Nucl. Instrum. Methods B **101**, 207 (1995).
[33] M. A. Henderson, A. Szabo, and J. T. Yates, Jr., J. Chem. Phys. **91**, 7245 (1989); Chem. Phys. Lett. **168**, 51 (1990).
[34] D. Y. Wesner, F. P. Coenen, and H. P. Bonzel, Phys. Rev. Lett. **60**, 1045 (1988).
[35] O. Knauff, U. Grosche, H. P. Bonzel, and V. Fritzsche, Mol. Phys. **76**, 787 (1992).
[36] G. Parshau and K. H. Rieder, Surf. Sci. **257**, L628 (1991).
[37] N. Pangher and J. Haase, Surf. Sci. **293**, L628 (1993).
[38] C. S. Feigerle, S. R. Desai, and S. H. Overbury, J. Chem. Phys. **93**, 787 (1990).
[39] T. Hertel, E. Knoesel, E. Hasselbrink, M. Wolf, and G. Ertl, Surf. Sci. **317**, L1147 (1994).
[40] P. Avouris, P. S. Bagus, and C. J. Nelin, J. Electron Spectrosc. Relat. Phenom. **38**, 269 (1986).
[41] P. S. Bagus and G. Pacchioni, Surf. Sci. **278**, 427 (1992).
[42] J. Rogozik, V. Dose, K. C. Prince, A. M. Bradshaw, P. S. Bagus, K. Hermann, and P. Avouris, Phys. Rev. B **32**, 4296 (1985).
[43] K. D. Tsuei and P. D. Johnson, Phys. Rev. B **45**, 4296 (1992).
[44] G. Blyholder, J. Phys. Chem. **68**, 2772 (1964).